Available online at www.sciencedirect.com

ScienceDirect

Energy Procedia 92 (2016) 199 – 204

Energy Procedia

6th International Conference on Silicon Photovoltaics, SiliconPV 2016

Parasitic absorption in polycrystalline Si-layers for carrier-selective front junctions

Sina Reiter[a], Nico Koper[a], Rolf Reineke-Koch[a], Yevgeniya Larionova[a], Mircea Turcu[a], Jan Krügener[b], Dominic Tetzlaff[b], Tobias Wietler[b], Uwe Höhne[c], Jan-Dirk Kähler[c], Rolf Brendel[a,d], Robby Peibst[a,b]

[a]*Institute for Solar Energy Research Hamelin (ISFH), Am Ohrberg 1, D-31860 Emmerthal, Germany*
[b]*Institute of Electronic Materials and Devices, Universität Hanover, Schneiderberg 32, D-30167 Hanover, Germany*
[c]*centrotherm pv AG, Vahrenwalder Str. 269A, D-30179 Hanover, Germany*
[d]*Institute for Solid State Physics, Leibniz Universität Hanover, Appelstraße 2, D-30167 Hanover, Germany*

Abstract

We investigate the optical properties of n- and p-type polycrystalline silicon (poly-Si) layers. We determine the optical constants *n* and *k* of the complex refractive index of polycrystalline silicon by using variable-angle spectroscopic ellipsometry. Moreover, we investigate the effect of different doping levels in the poly-Si on free carrier absorption (FCA). Thereby, we demonstrate that the FCA in poly-Si can be described by a model developed for crystalline silicon (*c*-Si) at a first approximation. The optical properties of hydrogenated amorphous silicon layers (*a*-Si:H) are also investigated as a reference. With ray tracing simulations the absorption losses of poly-Si and of the *a*-Si:H layers are quantified with respect to the film thickness. Based on this approach we find that the short-circuit current density losses due to parasitic absorption of poly-Si layers are significantly lower when compared to *a*-Si:H layers of the same thickness. For example the short-circuit current density loss due to a 20 nm thick p-type poly-Si layer is around 1.1 mA/cm^2, whereas a 20 nm thick p-type *a*-Si:H layer leads to a loss of around 3.5 mA/cm^2.

Peer review by the scientific conference committee of SiliconPV 2016 under responsibility of PSE AG.

Keywords: Polycrystalline silicon; optical properties; front junction; ray tracing simulations

1. Introduction

Carrier-selective based junctions between crystalline (*c*-) and polycrystalline (poly-) Si are currently attracting significant research interest. Recombination current densities down to 1 fA/cm^2 [1] and efficiencies up to 25.1 % [2] have been demonstrated with this approach. So far, the poly-Si layers have been mainly applied on the rear side of

Peer review by the scientific conference committee of SiliconPV 2016 under responsibility of PSE AG.
doi:10.1016/j.egypro.2016.07.057

the cell [2]. In the work of Römer *et al.* [3], 100 nm poly-Si were deposited on both sides of the cell, yielding a significant reduction of the short-circuit current density J_{sc} by parasitic absorption. Nevertheless, since the major limitation of today's industrial solar cells is recombination at the front side [4], it is desirable to utilize the excellent interface passivation of poly-Si/*c*-Si junctions. The purpose of this work is therefore to investigate the optical properties of poly-Si layers, and to determine constraints regarding thickness and doping level for an acceptable optical loss due to parasitic absorption.

2. Experimental details

We use single side-polished planar n-type Czochralski silicon wafers as substrate material. All substrates are prepared with a 220 nm thick oxide layer (SiO_2) grown in a wet oxidation process. The resulting layer thickness is determined by ellipsometry. Subsequently, we deposit intrinsic amorphous silicon layers on top of the oxide by using low pressure chemical vapor deposition (LPCVD). Next, ion implantation is applied to obtain different doping levels in the poly-Si layers. We implant phosphorus for n-type and boron for p-type poly-Si films, using doses of (0.2/1/5/7.5) $\times 10^{15}$ cm^{-2}, and (0.2/1/5) $\times 10^{15}$ cm^{-2}, respectively. Subsequently, the samples are annealed for 30 min (plateau) at 900 °C in a nitrogen atmosphere to form polycrystalline layers. Finally, the samples receive a 1 % HF dip for two minutes. The resulting poly-Si film thickness is about 145 nm. In addition, three samples with an approximately 50 nm-thick intrinsic, in situ n^+- or p^+-doped hydrogenated amorphous silicon layer on top of the SiO_2 are prepared by using plasma-enhanced chemical vapor deposition (PECVD) in a von Ardenne *CS 400P* cluster system.

We perform variable-angle spectroscopic ellipsometry measurements in the wavelength range of 240 nm to 1700 nm (M-2000UI from J.A. Woollam, Inc.) to determine the refractive index *n* and the extinction coefficient *k* as well as the different layer thicknesses of our samples.

3. Results and discussion

We measure the amplitude ratio Ψ and phase difference Δ of incident and reflected radiation for five angles of incidence (55°, 60°, 65°, 70°, 75°). Since we expect similar optical properties for *c*-Si and poly-Si, we first assemble a state-of-the-art optical model for the dielectric function $\varepsilon_{c\text{-}Si}(\lambda)$ of *c*-Si based on the combined dataset of Green (*n* values) [5] and Schinke *et al.* (*k* values) [6]. $\varepsilon_{c\text{-}Si}(\lambda)$ can be accurately described by five oscillators, whose parameters have been fixed in the following. These oscillators have been also used to describe the dielectric function $\varepsilon_{poly\text{-}Si}(\lambda)$ of poly-Si. The only extension of our model for $\varepsilon_{poly\text{-}Si}(\lambda)$ is the addition of one Drude term which describes the absorption by free carriers. The dielectric function of doped *a*-Si:H layers is modeled by employing a typical Cody–Lorentz optical model [7,8].

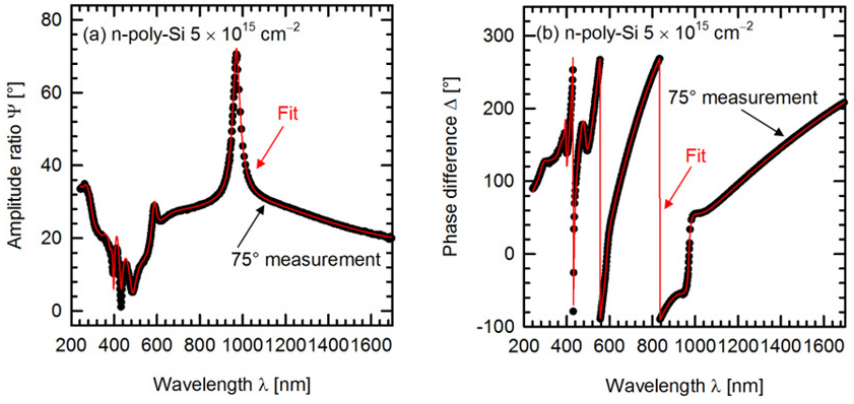

Fig. 1. Measured and modeled amplitude ratio Ψ (a) and phase difference Δ (b) plotted as a function of wavelength λ for a representative sample with an n-type poly-Si layer (implant dose 5×10^{15} cm^{-2}).

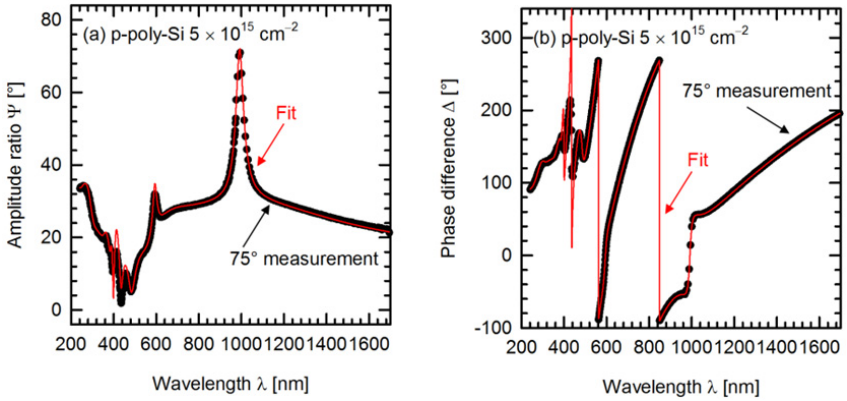

Fig. 2. Measured and modeled amplitude ratio Ψ (a) and phase difference Δ (b) plotted as a function of wavelength λ for a representative sample with a p-type poly-Si layer (implant dose 5×10^{15} cm^{-2}).

We use this model because the Cody-Lorentz model is supposed to take the interband absorption into account [9-11]. Figure 1 and Figure 2 exemplarily show the measured and modeled amplitude ratio Ψ and phase difference Δ for an n-type and p-type poly-Si layer implanted with a dose of 5×10^{15} cm^{-2}, respectively. This corresponds to the optimum value regarding the passivation quality of n-type poly-Si layers [1].

From our optical model for poly-Si, the optical constants *n* and *k* are extracted. We use the obtained *k* values to calculate the absorption coefficient $\alpha = 4\pi k/\lambda$ for all samples. Figure 3 shows the calculated absorption spectra for the differently doped poly-Si and *a*-Si:H layers. For comparison the *c*-Si absorption spectrum is also shown. As expected, the absorption spectra of the poly-Si layers exhibit similar features as that of *c*-Si between 300 nm and 800 nm. The different doping levels only affect the absorption coefficient at wavelengths above 800 nm. Here it can be noticed that the absorption coefficient increases with increasing doping level.

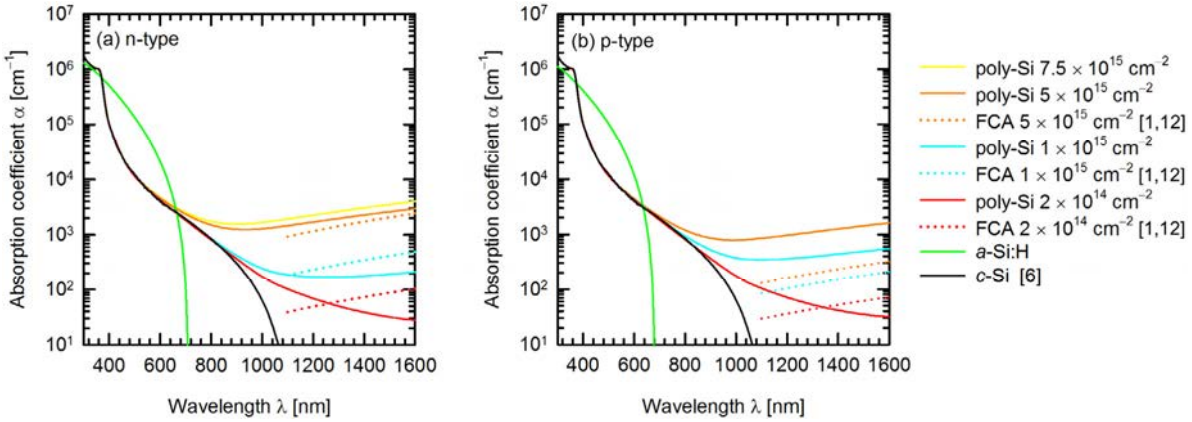

Fig. 3. Absorption coefficient α obtained by the extinction coefficient *k* from ellipsometry measurements for various n-doped poly-Si and *a*-Si:H (a) or p-doped poly-Si and *a*-Si:H layers (b).

We attribute this behavior to free carrier absorption. The dashed lines in Fig. 2(a,b) show that the order of magnitude of the free carrier absorption in poly-Si can be described by a parameterization developed for *c*-Si [12]. For the doping levels $(0.2/1/5)\times10^{15}$ cm^{-2} of poly-Si, we used the values that we measured by secondary ion mass spectroscopy (SIMS) [1], although these values refer to the total rather than to the active doping concentration.

According to Figure 3, the absorption losses due to poly-Si are significantly lower compared to *a*-Si:H layers up to 700 nm wavelength, which is promising with regards to silicon solar cells applications. Based on the results of optical parameters (*n*,*k*) mentioned above, we perform ray tracing simulations to determine the optical losses in a doped poly-Si or *a*-Si:H layer used as a front junction in a silicon solar cell. We use the program *Sunrays* [13] with an unit cell defined by a base area of (7.06 × 7.06) μm^2 and a *c*-Si wafer thickness of 150 μm. Centered on this structure a 5 μm high upright pyramid is located. On the rear side we assume perfect reflection properties with a Lamertian fraction Λ = 1 and a reflection coefficient *R* = 1. On the front side we assume two different layer stacks. On the one hand a stack consisting of *1.5nm SiO_2/ p- or n-poly-Si of layer thickness d/ 70nm SiN_x*, on the other hand a heterojunction system consisting of *5nm i-a-Si:H/ p- or n-a-Si:H of layer thickness d/ 70nm SiN_x*. For both solar cell types we only modify the thickness of the doped poly-Si or *a*-Si:H layer. A 150 μm-thick *c*-Si wafer covered with a 70 nm thick SiN_x layer and the same optical rear side properties is used as reference. It has a photogeneration that corresponds to a maximum the short-circuit current density $J_{sc}^*(0)$ = 42.70 mA/cm^2. Figure 4 shows the short-circuit density losses $\Delta J_{sc}^* = J_{sc}^*(0) - J_{sc}^*(d)$ as a function of the poly-Si or *a*-Si:H layer thickness *d*.

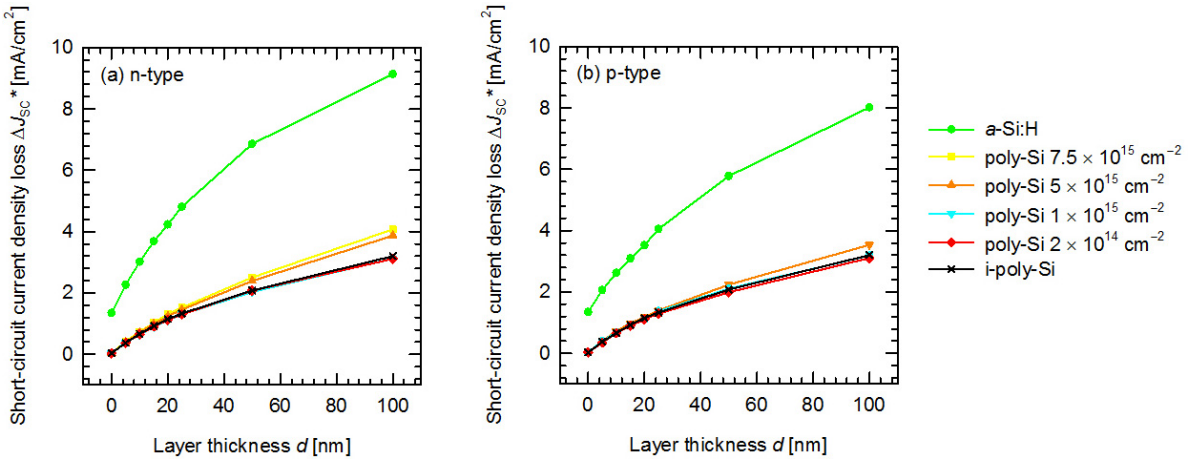

Fig. 4. Short-circuit current density losses ΔJ_{sc}^* due to parasitic absorption in n-doped poly-Si (a) and p-doped poly-Si layers (b). For comparison the short-circuit current density losses due to n- or p-doped *a*-Si:H is also shown. Notice that *a*-Si:H and poly-Si graphs don't start from the same origin. For a doped poly-Si (*a*-Si:H) layer of 0 nm thickness a 1.5 nm SiO_x (5 nm i-*a*-Si:H) layer is present.

The losses of J_{sc}^* increase with increasing layer thickness. Moreover, these losses are always more than twice as high for *a*-Si:H than for poly-Si layers of the same thickness. We observe larger losses in J_{sc}^* with increasing doping level due to enhanced free carrier absorption. With decreasing doping level the values converge towards the limit of intrinsic poly-Si within uncertainty limits. Figure 5(a) exemplarily shows the IQE and parasitic absorption spectra for a 20 nm-thick n-poly-Si layer. These spectra show that the main absorption losses result from the short and long wavelength regime. Taken together these results it should be possible to keep the optical losses in the poly-Si layer on the front side below 1 mA/cm^2 for layers up to 20 nm layer thickness.

In order to distinguish between parasitic absorption of high-energetic photons during the first pass through the poly-Si layer and parasitic absorption of low-energetic photons due to free carrier absorption during one of the numerous passes occurring at long wavelengths, we folded the internal quantum efficiency as determined with *Sunrays* with the AMG1.5 spectrum [14]. In accordance with Paviet-Salomon *et al.* [15], we distinguish between short-wavelength current density losses, corresponding to the wavelength integration range between 350 nm and 600 nm ($\Delta J_{sc\ short}^*$), and long-wavelength losses in the range 1000 nm – 1200 nm ($\Delta J_{sc\ long}^*$). Figure 5(b) exemplarily shows these loss contributions to the total loss ΔJ_{sc}^* for n-poly-Si implanted with a dose of 5×10^{15} cm^{-2}. The difference between the sum of $\Delta J_{sc\ short}^*$ and $\Delta J_{sc\ long}^*$ to ΔJ_{sc}^* originates from parasitic absorption in a wavelength regime between 600 nm and 1000 nm. It can clearly be seen that $\Delta J_{sc\ short}^*$ dominates the total loss ΔJ_{sc}^*, in particular for thin poly-Si layers.

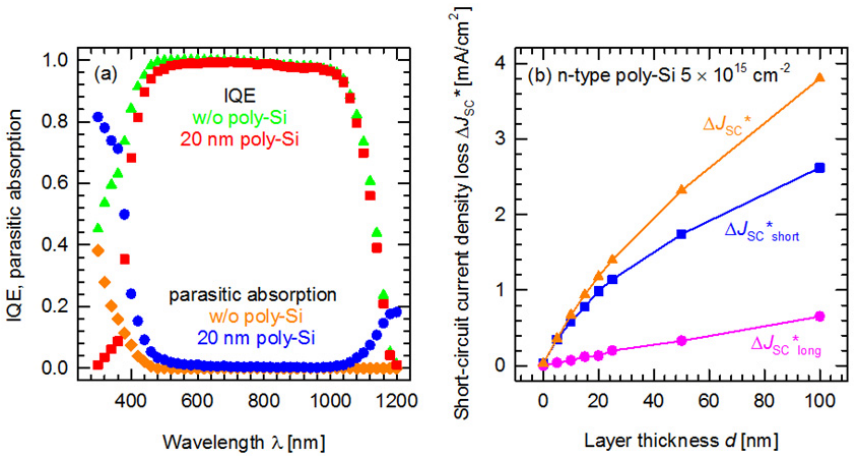

Fig. 5. (a) IQE and parasitic absorption spectra without poly-Si layer and with a 20 nm-thick n-poly-Si layer. (b) UV ($\Delta J_{sc\ short}^{*}$) and IR ($\Delta J_{sc\ long}^{*}$) loss contributions of total short-circuit current density losses ΔJ_{sc}^{*} for n-doped poly-Si (implant dose 5×10^{15} cm^{-2}).

4. Conclusion and outlook

In this work we measure the ellipsometric quantities Ψ and Δ in the regime of 240 nm to 1700 nm for several angles of incidence of differently n- and p-doped poly-Si layers. We model the dielectric function of poly-Si accurately on the basis of the dielectric function of *c*-Si extended by a Drude oscillator to describe the free carrier absorption in poly-Si. Subsequently, we extract the optical constants *n* and *k* from our optical model for poly-Si. The resulting absorption spectra show over a wide wavelength range lower absorption coefficients compared to n- and p-doped *a*-Si:H layers. The different doping levels of poly-Si affect the absorption coefficient at wavelengths above 800 nm so that the absorption coefficient increases with increasing doping level. Based on our optical parameters (*n*,*k*) we perform ray tracing simulations. We determine the optical losses in a doped poly-Si or *a*-Si:H layer used as a front junction. The losses of J_{sc}^{*} increase with increasing layer thickness and doping level. These losses are twice as high for *a*-Si:H than for poly-Si layers of the same thickness. These simulations show the possibility to keep the optical losses in doped poly-Si layers on the front side below 1 mA/cm^2 for layer thicknesses up to 20 nm. Nevertheless, our investigation demonstrates the optical advantages of poly-Si compared to *a*-Si:H layers and the high potential for silicon solar cell applications. Another option the increase the transparency even further are oxygen-doped semi-insulating polycrystalline silicon (SIPOS) layers [16-18]. This material is also used for electrical passivation and solar cell applications [17,18]. The optical and electronic properties depend on the oxygen content of these films and can be easily adjusted [16-18].

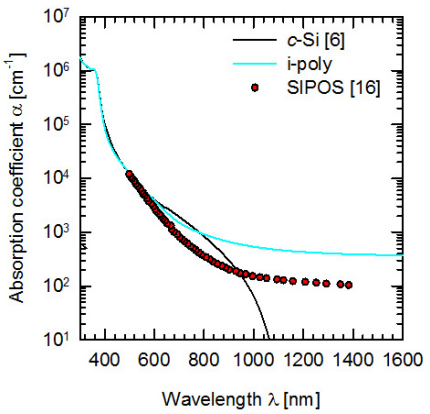

Fig. 6. Absorption coefficient α for *c*-Si, intrinsic poly-Si and an SIPOS layer annealed at 1000 °C.

The absorption coefficient α of a SIPOS layer in comparison to *c*-Si and intrinsic poly-Si is shown in figure 6. Between 500 nm and 1000 nm (a range of particular relevance), the absorption coefficient of SIPOS is significantly lower than that of pure poly-Si and *c*-Si. Work in this direction is under way.

Acknowledgement

This work is financially supported by the Federal Ministry for Economic Affairs and Energy (BMWi) under contact number 0325702.

References

[1] Römer U, Peibst R, Ohrdes T, Lim B, Krügener J, Wietler T, Brendel R. Ion implantation for poly-Si passivated back-junction back-contacted solar cells. IEEE 2015;5(2):507-514.
[2] Glunz SW, Feldmann F, Richter A, Bivour M, Reichel C, Steinkemper H, Benick J, Hermle M. The irresistible charm of a simple current flow pattern – 25% with a solar cell featuring a full-area back contact. Proceedings of the 31st European Photovoltaic Solar Energy Conference and Exhibition 2015;259-263.
[3] Römer U, Peibst R, Ohrdes T, Lim B, Krügener J, Bugiel E, Wietler T, Brendel R. Recombination behaviour and contact resistance of n^+ and p^+ poly-crystalline Si/mono-crystalline Si junctions. Solar Energy Materials and Solar Cells 2014;131:85-91.
[4] Brendel R, Dullweber T, Peibst R, Kranz C, Merkle A, Walter D. Breakdown of the efficiency gap to 29% based on experimental input data and modelling. Proceedings of the 31st European Photovoltaic Solar Energy Conference and Exhibition 2015;264-272.
[5] Green MA. Self-consistent optical parameters of intrinsic silicon at 300 K including temperature coefficients. Solar Energy Materials and Solar Cells 2008;92:1305-1310.
[6] Schinke C, Peest PC, Schmidt J, Brendel R, Bothe K, Vogt MR, Kröger I, Winter S, Schirmacher A, Lim S, Nguyen HT, MacDonald D. Uncertainty analysis for the coefficient of band-to-band absorption of crystalline silicon. AIP Advances 2015;5:067168.
[7] Ferlaut AS, Ferreira GM, Pearce JM, Wronski CR, Collins RW. Analytical model for the optical functions of amorphous semiconductors from the near-infrared to ultraviolet: Applications in thin film photovoltaics. Journal of Applied Physics 2002;92:2424.
[8] Rothfelder M, Bläsi B, Peters M, Künle M, Janz S. Using spectroscopic ellipsometry for the characterisation of thin films for advanced photovoltaic concepts. Proceedings of the 24th European Photovoltaic Solar Energy Conference and Exhibition 2009;270-275.
[9] Papaferri D. Dissertation.Manufacturing and characterization of amorphous silicon alloys passivation layers for silicon heterojunction solar cells. University of Bologna, 2013.
[10] Ferlauto AS, Ferreira GM, Pearce JM, Wronski CR, Collins RW, Deng X, Ganguly G, J. App. Phys. 2002;92:2424.
[11] Cody GD. Semiconductors and Semimetals (edited by J. I. Pankove). Academic Press. 1984; 21B:11.
[12] Rüdiger M, Greulich J, Richter A, Hermle M. Parameterization of free carrier absorption in highly doped silicon for solar cells. IEEE 2013;60 (7):2156-2162.
[13] Brendel R. Sunrays: a versatile ray tracing program for the photovoltaic community. Proceedings of the 12th European Photovoltaic Solar Energy Conference 1994.
[14] IEC 60904-3 (Ed. 2), Photovoltaic devices – Part 3: Measurement principles for terrestrial photovoltaic (PV) solar devices with reference spectral irradiance data. 2008.
[15] Paviet-Salomon B, Tomasi A, Descoeudres A, Barraud L, Nicolay S, Despeisse M, De Wolf S, Ballif C. Back-contacted silicon heterojunction solar cells: optical-loss analysis and mitigation. IEEE 2015;5(5):1293-1303.
[16] Kwark Y, Swanson RM. Optical absorption of thin SIPOS films. Journal of The Electrochemical Society 1982;129:197-201.
[17] Pan Y, Wang Y. Study on the optical absorption of oxygen-doped polysilicon thin films. Optical Engineering 1993;32 (3):589-592.
[18] Brüesch P, Stockmeier T, Stucki F, Buffat PA. Physical properties of semi-insulating polycrystalline silicon. 1. Structure, electronic properties, and electrical conductivity. Journal of Applied Physics 1993;73:7677.